



Originally published as:

Förster, S., Kaden, K., Foerster, M., Itzerott, S. (2012): Crop type mapping using spectral-temporal profiles and phenological information. - *Computers and Electronics in Agriculture*, 89, 30-40

DOI: [10.1016/j.compag.2012.07.015](https://doi.org/10.1016/j.compag.2012.07.015)

1 Crop type mapping using spectral-temporal profiles and phenological in- 2 formation

3

4 Saskia Foerster^{1*}, Klaus Kaden², Michael Foerster³, Sibylle Itzerott¹

5 ¹ Section Remote Sensing, Helmholtz Centre Potsdam GFZ German Research Centre for Ge-
6 osciences, Telegrafenberg, 14473 Potsdam, Germany; foerster@gfz-potsdam.de,
7 itzerott@gfz-potsdam.de

8 ² Institute for Earth and Environmental Sciences, University of Potsdam, K.-Liebknecht Str.
9 24-25, 14476 Potsdam-Golm, Germany; kkaden@uni-potsdam.de

10 ³ Institute for Landscape Architecture and Environmental Planning, TU Berlin, Str. d. 17. Juni
11 145, 10623 Berlin, Germany; michael.foerster@tu-berlin.de

12

13 * Corresponding author. Tel.: +49 (0)331 288 28615, Fax: +49 (0)331 288 1192, E-mail ad-
14 dress: foerster@gfz-potsdam.de.

15

16 Abstract

17 Spatially explicit multi-year crop information is required for many environmental applica-
18 tions. The study presented here proposes a hierarchical classification approach for per-plot
19 crop type identification that is based on spectral-temporal profiles and accounts for deviations
20 from the average growth stage timings by incorporating agro-meteorological information in
21 the classification process. It is based on the fact that each crop type has a distinct seasonal
22 spectral behaviour and that the weather may accelerate or delay crop development. The classi-
23 fication approach was applied to map twelve crop types in a 14 000 km² catchment area in
24 Northeast Germany for several consecutive years. An accuracy assessment was performed
25 and compared to those of a maximum likelihood classification. The 7.1 % lower overall clas-

26 sification accuracy of the spectral-temporal profiles approach may be justified by its inde-
27 pendence of ground truth data. The results suggest that the number and timing of image ac-
28 quisition is crucial to distinguish crop types. The increasing availability of optical imagery
29 offering a high temporal coverage and a spatial resolution suitable for per-plot crop type map-
30 ping will facilitate the continuous refining of the spectral-temporal profiles for common crop
31 types and different agro-regions and is expected to improve the classification accuracy of crop
32 type maps using these profiles.

33

34 Key words: crop type mapping, NDVI temporal profiles, multi-temporal, phenological correc-
35 tion, agro-meteorological data

36

37 **1 Introduction**

38

39 Timely availability of large-scale information on the spatial distribution of crop types is re-
40 quired to support modeling and managing of agro-environmental systems from regional to
41 national scales. Often this information is only available as averages at the level of administra-
42 tive units and is usually not obtainable for areas with deviating boundaries, e.g. river basins
43 (De Witt and Clevers, 2004). Many agro-environmental applications such as agricultural
44 flood damage estimation or water quality modeling, however, require spatially distributed
45 crop data.

46 For these applications remote sensing is nowadays an important source of information
47 (Vincikova et al., 2010). Due to the dynamic character of agricultural systems, crop type
48 mapping based on multi-temporal approaches is superior over single-date image analyses.
49 While traditional approaches using parametric or non-parametric classification algorithms re-
50 quire ground truth data to train the classifier (e.g., Yang et al., 2011; Castillejo-González et

51 al., 2009), the use of crop-specific spectral-temporal profiles is independent of ground truth
52 data. The independence of ground truth data nevertheless facilitates operational monitoring of
53 agricultural land use over large areas and longer time periods.

54 The use of spectral-temporal profiles for crop identification by satellite data was first pro-
55 posed in the 1980s. Odenweller and Johnson (1984) presented characteristic profiles observed
56 for a variety of crops by use of a vegetation indicator that measures the infrared reflectance
57 relative to the reflectance in the visible range. The term ‘spectral-temporal profile’ refers to
58 the spectral behaviour of a certain crop type throughout the year. Profile-based crop identifi-
59 cation is based on the fact that profiles representing a specific crop are usually more similar
60 than profiles representing different crops (Odenweller and Johnson, 1984). Several studies
61 investigated the use of crop-specific seasonal profiles for crop discrimination and mapping at
62 different spatial scales from local to state level (Wardlow et al., 2007; Murthy et al., 2003;
63 Sakamoto et al., 2005; Jakubauskas et al., 2002). Most of the studies are based on temporal
64 profiles of the Normalized Difference Vegetation Index (NDVI) as an effective indicator of
65 the photosynthetically active vegetation (e.g., Bradley et al., 2007; Wardlow and Egbert,
66 2008). The NDVI is the most commonly used vegetation index applied in agricultural applica-
67 tions, however, several other vegetation indices have been proposed to reduce the influence of
68 the canopy background and the atmosphere (Reed et al., 2003), such as the Soil Adjusted
69 Vegetation Index (SAVI, Huete, 1988) or the Enhanced Vegetation Index (EVI, Huete et al.
70 1997). The NDVI is a measure of photosynthetic capacity of the vegetation cover, while the
71 SAVI is more suitable to reflect the vegetation canopy structure (Reed et al., 2003). The EVI
72 was found to be more sensitive to variations over high biomass areas, e.g. forests, when the
73 NDVI tended to saturate (Huete et al., 2002). Furthermore, EVI may be advantageous in areas
74 with high humidity since it is designed to minimize the effects of the atmosphere. Huete et al.
75 (1997) conclude that each index had its strengths and weaknesses for certain applications.

76 Depending on the application at hand, satellite imagery ranging from low to high spatial reso-
77 lution is applied for studying agricultural landscapes (Vincikova et al., 2010). For per-field
78 crop type mapping, the spatial resolution of the imagery should be chosen relative to the typi-
79 cal field size. Apart from an adequate spatial resolution, the temporal resolution of the satel-
80 lite data is critical for crop discrimination and mapping. Several authors have studied optimal
81 times of image acquisition with respect to the growing stages (Murakami et al., 2001; Van
82 Niel and McVicar, 2004).

83 The appearance of crop profiles is affected by regional variations in climate and management
84 practices, which should be accounted for by setting-up individual crop profiles for each ho-
85 mogenous agro-region (Wardlow et al., 2007). Crop profiles, however, also vary from year to
86 year resulting from specific weather conditions and, in particular, deviations in the tempera-
87 ture and precipitation distribution throughout the growing season (Siebert and Ewert, 2012).
88 These inter-annual variations have so far hardly been accounted for in crop type mapping ap-
89 proaches.

90 In this study we therefore propose an efficient hierarchical classification algorithm that is
91 based on spectral-temporal profiles of crop types and accounts for weather-induced inter-
92 annual variations in the spectral-temporal behaviour through the use of agro-meteorological
93 information. The proposed approach was tested using multi-temporal LANDSAT satellite im-
94 agery for the per-field crop type mapping of a large lowland river catchment in Germany.

95

96 **2 Data basis and pre-processing**

97 To set up characteristic temporal profiles for each crop, NDVI data from a sixteen year satel-
98 lite image time series were combined with cultivation data collected from farming companies
99 for the same time period and agro-meteorological data provided by the weather service. The

100 spectral-temporal profiles were then used to map crop types in the study area, the Havel River
101 catchment, for the years 1994-2000 utilizing agro-meteorological data from the same period.
102 The study area is located in the north east of Germany (Figure 1). It comprises the catchment
103 of the Havel River, a tributary of the Elbe River, excluding the Spree catchment, and covers a
104 total area of 14 000 km². Arable land is the dominant land use covering 37.7 % of the total
105 area. Soils are predominantly sandy with areas of high and low ground water. The average
106 plot size is 21 ha. Major crops are winter rye (15 %), winter wheat (12 %), maize (12 %) and
107 oilseed rape (10 %) (Amt fuer Statistik Berlin Brandenburg, 2010).

108

109 < Figure 1 >

110

111 **2.1. Crop cultivation data**

112 Cultivation data from the years 1987 to 2002 of 424 agricultural plots with a total area of
113 9021 ha were collected from six agricultural companies in the study area. More specifically,
114 for each of these 424 plots information on the specific crops grown in the years of satellite
115 image data acquisition was made available, resulting in a total of 3745 reference plot data
116 (Table 1). These data served the development of the spectral-temporal profiles and were used
117 to validate the final crop type map.

118 For the per-plot crop type mapping, a data set of the agricultural plots present in the study ar-
119 ea is required in order to exclude other land use types from the classification process and ena-
120 ble a crop type identification at the plot level. This plot map may be either derived from offi-
121 cial land cover data sets or from object-based image analysis (Blaschke, 2010). For our study
122 area a digital land cover data set based on mapping CIR aerial photographs was available
123 from the state ministry of environment.

124

125 < Table 1 >

126

127 **2.2. Satellite image time series**

128 Spectral information from 35 LANDSAT TM/ETM images acquired between the years 1987
129 and 2002 was used to set up the temporal crop type profiles. The image acquisition dates are
130 listed in Table 2. LANDSAT images were chosen for this study for different reasons. They
131 are available for several years to decades and are therefore suitable for long-term monitoring
132 studies (Wulder et al., 2008). The spatial resolution of 30 m allows for single plot crop type
133 identification and the image size of approximately 175 by 175 km encompasses the whole
134 study area. The repetition rate of 16 days results in approximately two to five cloud-free
135 coverages of our study area per year. The LANDSAT images were atmospherically and geo-
136 metrically corrected to allow for multi-temporal analyses (Richter, 1996) and the NVDI was
137 then computed for each image. We chose the most commonly used NDVI for this study, since
138 our agricultural study area in Central Europe is characterized by low biomass and no particu-
139 larly high humidity..

140

141 **2.3. Agro-meteorological data**

142 The different crop types undergo certain specific growth stages and agro-technical treatments
143 throughout the growing season. These are for the example of cereals, sowing, seedling
144 growth, tillering, stem elongation, flowering, grain-fill period (milk and dough development),
145 ripening and harvest. As a result of specific weather patterns throughout individual years, par-
146 ticularly the temperature and precipitation characteristics, the onset and duration of the growth
147 stages and the times of agro-technical treatments may deviate from an average year. Depend-
148 ing on the demands of the individual crop types, the timing not only differs among certain
149 years but also among the individual crops in the same year. Growth stage timings in the study

150 area can deviate up to approximately 20 days in both directions, i.e. ahead or behind the aver-
151 age development. To account for these deviations, agro-meteorological data were incorpo-
152 rated in the process of setting up spectral-temporal profiles and in the crop type classification.
153 Nowadays many weather services provide such agro-meteorological data. For our study we
154 used data made available by the German Weather Service (Deutscher Wetterdienst - DWD,
155 www.dwd.de) for the period 1951-2003 collected at 40 stations within our study area. They
156 contain information on times of growth stages, e.g. the onset of flowering, and agro-technical
157 treatments for most common crop types in each year. Based on these data we calculated the
158 average day of the year of each of these stages to obtain the average phenological pattern for
159 each individual crop type present in the study area.

160

161 < Table 2 >

162

163 **3 Methods**

164 **3.1 Spectral-temporal profiles of crop types including phenological correction**

165

166 The spectral-temporal profiles represent the average phenological behaviour of each of the
167 twelve most commonly grown crop types in North Germany. These comprise winter rye, win-
168 ter wheat, winter barley, oilseed rape, sugar beets, maize, summer grain, potatoes, oilseed
169 crops and legumes, first year and perennial field grass and fallow land. Based on the dates of
170 image acquisition of the 35 LANDSAT images collected between the years 1987 and 2002,
171 for each crop type the phenological day was determined according to the agro-meteorological
172 information. Different from the actual day of the year, the term ‘phenological day’ refers to
173 the phenological stage of a crop type in a certain year as a result of the temperature and pre-
174 cipitation pattern in that specific year. The phenological correction is shown schematically in

175 Figure 2. Dotted and dashed lines represent the deviation in days for two individual crop types
176 and two different years as compared to the average year. The average is derived from the
177 mean timings of the growth stages based on the agro-meteorological data from the weather
178 service of the years 1951-2003. In the hypothetical Year 1, unfavourable temperature and pre-
179 cipitation conditions in spring may have led to a delay as compared to the average NDVI de-
180 velopment. In the course of the year the lines slowly approach the average line as the delay
181 reduces. Conversely, in the hypothetical Year 2 crop development in spring is ahead of the
182 average due to favourable weather conditions, while in the later course of the year the crop
183 development lags behind the average. The deviation among individual crop types in the same
184 year is due to the crop types' different weather tolerability.

185

186 < Figure 2 >

187

188 The resulting list of phenologically corrected dates was combined with the average NDVI
189 values for each of the 3745 agricultural reference plots. Subsequently, for each crop type the
190 seasonal NDVI was plotted and studied in regard to its average development and variability
191 throughout the season. While natural vegetation is characterized by a relatively continuous
192 seasonal NDVI development, the seasonal NDVI of arable lands decreases more abruptly due
193 to agro-technical treatments such as harvesting or mowing. These distinct NDVI declines are
194 characteristic for each crop type and must therefore be contained in the individual NDVI tem-
195 poral profiles. The final spectral-temporal profiles were then generated by interpolating the
196 average NDVI values while retaining the characteristic decline features.

197

198 **3.2 Crop type mapping by hierarchical classification**

199 Once the NDVI temporal profiles are set up they can be used to map crop types for any year
200 without the need of additional ground truth data. The study area should be located in the same
201 broad agro-region to ensure transferability of the profiles.

202 A two-level hierarchical classification scheme was implemented. At the first level the three
203 broad groups of summer crops, winter crops and perennial field grass / fallow land were clas-
204 sified. To separate perennial field grass / fallow land from the other two groups, those pixels
205 that had high NDVI values in all available images throughout the growing season were classi-
206 fied as belonging to this group. Using a majority filter, the respective plots were excluded
207 from the subsequent separation of summer and winter crops. This separation was based on
208 two images, one acquired in winter / early spring and a second acquired in late spring / sum-
209 mer. While winter crops exhibit high NDVI values in both images, summer crops are charac-
210 terized by a large difference in NDVI between both images with low values in winter / early
211 spring and high values in late spring / summer. Again, a majority filter was used to assign the
212 broad groups to the respective plots. As a result we obtained three separate masks containing
213 plots with summer crops, winter crops and perennial field grass / fallow land.

214 At the second level single crop types within the three groups were classified based on their
215 NDVI temporal profiles. For each date of image acquisition and each crop type, the
216 phenological date, i.e. the day of the year corresponding to the actual phenological stage, was
217 determined based on the agro-meteorological data. From the temporal profiles NDVI infor-
218 mation was extracted for these phenologically corrected dates of image acquisition. This in-
219 formation was then used in the pixel-based classification using parallelepiped classification.
220 The classification thresholds were defined by the standard deviation of the NDVI temporal
221 profiles for each crop type and date. In cases of class overlap a minimum distance algorithm
222 was applied using the image in which the classes to be separated show the largest difference
223 in NDVI. In cases when the pixel was not within the thresholds, these were iteratively in-

224 creased. Finally, the classification results were combined in a joint crop type map. Using a
225 majority filter, the dominant crop type per plot based on the plot boundaries was determined
226 and assigned to each plot to derive the final crop type map for a certain year.

227 Additionally, a traditional maximum likelihood classification based on the same satellite im-
228 agery and on ground truth data was performed in order to assess the quality of the new classi-
229 fication algorithm based on NDVI temporal profiles.

230

231 **4 Results**

232 For each of the crop types the seasonal NDVI was plotted as exemplarily presented for winter
233 rye and maize in Figures 3 and 4, respectively. The box plots show the variance of the NDVI
234 values for each image acquisition date, while only those dates are included that have more
235 than ten values. The NDVI exhibits a distinct seasonal pattern throughout the year with high-
236 est values between days 120 and 130 (early May) for winter rye and around 230 (mid August)
237 for maize. The variability of NDVI values varies throughout the year and among different
238 crops. For winter rye, the variability is largest during times of tillering until approximately
239 day 115 (mid April) and after harvest from day 220 (early August) onwards, while it is small-
240 est between days 115 (mid April) and 150 (end of May) during times of stem elongation and
241 between days 200 (mid July) and 210 (end of July) during times of yellow-ripe. Maize shows
242 a less distinct seasonal behaviour regarding NDVI variability. This can be attributed to the
243 fact that maize shows a stronger dependence on the local soil and groundwater conditions,
244 which the phenological correction does not account for. Hence the NDVI variability is higher
245 throughout the year and the NDVI development is less continuous as compared to winter rye.

246

247 < Figure 3 >

248 < Figure 4 >

249

250 The spectral-temporal profiles for each of the 12 major crop types generated from the NDVI
251 data can be clustered into three phenological groups (Figures 5 to 7). These are winter crops,
252 summer crops and perennial field grass / fallow land. Among the groups each profile is spe-
253 cific in respect to the onset and duration of growth stages and agro-technical treatment times,
254 the length of the growing period and the amount of photo-synthetically active vegetation pre-
255 sent at the plots throughout the year.

256

257 < Figure 5, in colour >

258 < Figure 6, in colour >

259 < Figure 7, in colour >

260

261 Winter crops such as winter wheat and oilseed rape are sown in autumn. Accordingly, the
262 NDVI values are characterized by a first increase in autumn and a second rapid increase in
263 spring until reaching a maximum in early summer that is followed by a rapid decrease during
264 the maturity stage in which harvesting and mowing dates are clearly distinguishable. Oilseed
265 rape shows a characteristic temporary drop in NDVI values in May due to flowering.

266 Different from winter crops, summer crops are sown in spring and were therefore separable
267 using spring images in the classification process. For other summer crops such as potatoes,
268 maize and sugar beets, the increase in NDVI values starts only in mid May. While potatoes
269 have a comparably short phenological cycle with a rapid NDVI decrease due to leaf senes-
270 cence during maturing, sugar beets are characterized by high NDVI values until late October.

271 Fallow land and perennial field grass exhibit high NDVI values throughout the year with less
272 variation as compared to summer and winter crops. Abrupt decreases in NDVI are due to

273 mowing in the case of perennial field grass and the natural annual cycle of growth and wither-
274 ing in case of the natural vegetation on fallow land.

275 The presented hierarchical classification algorithm based on the generated NDVI temporal
276 profiles was applied to map crop types in the study area for seven consecutive years 1994-
277 2000. For each year two to five satellite images were available (cf. Table 2). Figure 8 shows
278 the resulting crop type map of the entire study area for the year 2000. The distribution of the
279 predominant crop types reflects the pattern of soil quality and water availability. On the sandy
280 nutrient-poor areas, fallow land and winter rye predominate, while in the lowland areas with
281 high soil quality and good water availability maize is the dominant crop type. Figure 9 pre-
282 sents crop type maps for a subset area of approximately 30 by 30 km for the years 1994-2000.
283 Mapping crops of consecutive years allows the study of crop rotation patterns. We found that
284 there are no fixed crop rotations, which was confirmed by the farmers.

285

286 < Figure 8, in colour >

287 < Figure 9, in colour >

288

289 A per-plot accuracy assessment was performed for the crop type map of the growing season
290 1994/1995, based on 144 agricultural plots comprising an overall area of 1°620°ha. For this
291 growing season four satellite images were available (Table 3). Thus, the winter crops were
292 represented by four images, while the summer crops were represented by three images. Table
293 3 also lists the phenologically corrected days of the year that were used in the classification
294 process for each of the twelve crop types and each image.

295

296 < Table 3 >

297

298 The results of the accuracy assessment are summarized in Table 4. It presents the errors of
299 commission (user's accuracy), omission (producer's accuracy), and the overall accuracy. The
300 error of omission is the proportion of agricultural plots (given in hectare and percent) that is
301 not correctly identified as belonging to a particular crop class. The error of commission is the
302 proportion that is incorrectly identified as belonging to a particular class. The overall accuracy
303 gives the proportion of correctly classified plots relative to the total number of validation
304 plots. The overall accuracy was found to be 65.7 %. When interpreting this number, one has
305 to bear in mind that the classification algorithm is transferable, i.e. no ground truth data are
306 required in the classification process, and that the large number of twelve different crop types
307 were distinguished. When summarizing the results at the hierarchical level of summer crops,
308 winter crops and perennial field grass / fallow the overall accuracy increases to 86.3 %. While
309 winter crops were classified with a high accuracy of 91.9 %, only 83.1 % of the summer crop
310 plots were correctly classified. This may be primarily due to the different number and timings
311 of images available for classifying summer and winter crops, while the information content of
312 the July and August images is similar in regard to class separability. The misclassification be-
313 tween winter and summer crops at the first level of the hierarchical classification can be
314 mainly attributed to the fact that an early spring image was not available in that particular
315 growing season.

316 Highest crop-specific accuracies were obtained for winter wheat (91.7 %), oilseed rape
317 (97.3 %) and oilseed crops and legumes (92.1 %), while moderate accuracies of more than
318 70 % were obtained for fallow land, winter barley and winter rye. Most of the classification
319 error was associated with potatoes, sugar beets and maize. Only 14.5 % of maize plots were
320 correctly classified, while 68.5 % were misclassified as being potatoes. Sugar beets were
321 completely misclassified as being oilseed crops and legumes. This misclassification may be
322 partly attributed to the unfavourable image acquisition dates, when a September image would

323 allow a better differentiation between these crops. Furthermore, the end of July and early Au-
324 gust 1995 were characterised by exceptionally low precipitation rates, leading to a negative
325 water balance in the study area. The water stress led to a rapid withering of maize leaves in
326 sandy locations with low groundwater making them appear spectrally similar to withered po-
327 tato leaves. Maize that is cultivated in lowland areas with good access to groundwater does
328 not show the withering phenomenon and is correctly classified as maize.

329

330 < Table 4 >

331

332 To assess the quality of the classification algorithm based on NDVI temporal profiles, a tradi-
333 tional maximum likelihood classification using the same four satellite images was performed.
334 The results of the accuracy assessment are summarized in Table 5. With 72.8 % the overall
335 accuracy was found to be higher as compared to the classification based on NDVI temporal
336 profiles. This expected increase in classification accuracy can be attributed to the fact that the
337 maximum likelihood classification is based on ground truth data and therefore the classifier is
338 adjusted to the specific image statistics. When comparing the error matrices of both classifica-
339 tion approaches (Table 4 and 5) similarities become apparent. In both approaches most classi-
340 fication error was associated with summer crops suggesting that the availability of images has
341 a larger influence on the final result as compared to the type of classifier.

342

343 < Table 5 >

344

345 **5 Discussion and conclusions**

346 The classification approach proposed in this study allows an effective crop type mapping for
347 large areas and several consecutive years. It can facilitate various environmental applications

348 that require spatially explicit multi-year crop information such as water quality modeling
349 (Krysanova et al., 1998) or agricultural flood loss estimation (Pantaleoni et al., 2007).

350 The hierarchical classification algorithm for per-plot crop type identification is based on dis-
351 tinct spectral-temporal profiles and accounts for inter-annual weather variations by incorpo-
352 rating agro-meteorological information in the classification process. The classification ap-
353 proach was applied to map twelve crop types in a 14 000 km² catchment in Northeast Germa-
354 ny for several consecutive years. Several recent crop mapping studies that compared the accu-
355 racy of supervised classification methods found the maximum likelihood classifier to perform
356 best (Yang et al., 2011; Castillejo-Ganzález et al., 2009). Therefore the accuracy of the crop
357 type mapping based on the spectral-temporal profiles was compared to that of a maximum
358 likelihood classification (MLC). The overall accuracy increased from 65.7 % using the NDVI
359 temporal profiles approach to 72.8 % using the ML classifier. While the MLC is based on
360 training sets for each image used in the classification process, the NDVI temporal profiles ap-
361 proach is independent of ground truth data and solely requires information on the
362 phenological stages of the individual crops at the time of image acquisition. The independ-
363 ence of ground truth data and therefore the transferability may justify the 7.1 % lower overall
364 classification accuracy of the classification approach based on NDVI temporal profiles.

365 There are two major reasons for the slightly lower accuracy. These are the number and timing
366 of image acquisitions and the occurrence of exceptional weather conditions. The classification
367 based on the spectral-temporal profiles is more sensitive to the image acquisition dates than
368 the MLC. This fact is illustrated by the confusion of summer grain and winter wheat in the
369 growing season 1994/95 (cf. Tab. 4). The only major difference between the two spectral-
370 temporal profiles is the later onset of NDVI increase of summer grain (around day 100) as
371 compared to winter wheat (around day 70). If no image from this period is available, the clas-
372 ses will be confused. For the separability of all twelve crop type classes, the number and ac-

373 quisation date of the images is therefore crucial. Optimal acquisition periods are those that al-
374 low the highest differentiation between crops, but are not necessarily peak growth times
375 (Panigrahy and Sharma, 1997). For our study area these optimal acquisition periods were
376 found to be early/mid April, mid May, early July, mid August and mid September. The se-
377 cond major reason for the slightly lower accuracies achieved with the spectral-temporal pro-
378 file approach is the occurrence of unusual weather conditions, such as periods of exception-
379 ally high or low temperature or precipitation that lead to strong deviations from the average
380 spectral-temporal profiles for certain crop types in certain years. These deviations are particu-
381 larly due to drought stress or changes in cultivation practices as a result to these weather con-
382 ditions. They are not accounted for by the phenological correction using the agro-
383 meteorological data, because this correction only implies a temporal shift of the spectral-
384 temporal curve, but no modification in its shape or height. If the height of the profile strongly
385 deviates from the average, e.g., due to exceptionally low NDVI values during drought condi-
386 tions or some major management practices such as an earlier harvest, the spectral-temporal
387 profile approach fails to classify correctly. One example for such an event is the summer
388 drought period in 1994/95 that led to a rapid leave withering of (the water demanding crop)
389 maize.

390 In both cases, i.e. if images of optimal acquisition periods are missing or the spectral-temporal
391 profile is extremely deviating from the average, the accuracy of the spectral-temporal profiles
392 approach is expected to be lower as compared to the MLC. This is due to the fact that the
393 MLC uses image spectral information for a statistical adaption, while the spectral-temporal
394 profile approach is solely relying on the average annual behaviour of the NDVI. Figure 10
395 compares the overall accuracy of both classification approaches for all twelve crop type clas-
396 ses for the growing season 1994/95. While the misclassification of summer grain and sugar
397 beets using the spectral-temporal profiles approach can be mainly attributed to unfavourable

398 image acquisition dates (missing early spring and September images, respectively), the mis-
399 classification of maize can be mainly explained as a result of the water stress maize plants at
400 sandy locations experienced during the drought period in July and August of 1995. Figure 10
401 also shows that in the growing season 1994/95 for most crop types, i.e. fallow, perennial field
402 grass, winter crops, oilseed rape, potatoes, and first year field grass, the results of the spectral-
403 temporal profiles classification is comparable and even slightly better (by 0.6 % overall accu-
404 racy) as compared to the MLC. In case of the oilseed crops and legumes, the spectral-
405 temporal profiles classification outperforms the MLC by 49 %, because in the MLC oilseed
406 crops and legumes are often confused with perennial field grass. This points out the advantage
407 of a hierarchical approach used in the spectral-temporal profile classification that separated in
408 a first step perennial field grass and fallow land from summer and winter crops based on their
409 high NDVI values throughout the year.

410

411 < Figure 10 >

412

413 The generated spectral-temporal profiles are only valid within one agro-region, i.e. a region of
414 similar characteristics with regard to climate, soil and agro-technical conditions, and need to
415 be adapted when applied to other agro-regions. However, even within an agro-region crops
416 may develop differently depending on the soil and groundwater conditions, which may lead to
417 misclassifications. While some crop types are characterized by a distinct continuous seasonal
418 NDVI curve with low variation across the study area such as shown at the example of winter
419 rye (Figure 3), other crop types such as maize (Figure 4) show a high variability across the
420 study area as a result of its strong dependency on soil and groundwater conditions. Hence, the
421 spectral-temporal profile is not valid for maize grown at different conditions. This suggests
422 that the classification accuracy may be further improved by the inclusion of additional *a-*

423 *priori* information on the cultivation suitability for certain crop types such as soil quality or
424 water availability. Apart from the spatial variation in crop phenology within and among dif-
425 ferent agro-regions, also a temporal development in crop phenology over the last few decades
426 can be observed. Siebert and Ewert (2012) found out that the average temperature increase in
427 Germany in the last 50 years resulted in an earlier onset and shortening of most phenological
428 stages of oat. According to their study, the length of the growing season of oat in Germany
429 decreased by about two weeks between 1959 and 2009. Consequently, the spectral-temporal
430 profiles of crop types are subject to both spatial and temporal variations.

431 The further development of the proposed spectral-temporal profiles approach will benefit
432 from the recent rapid increase in the availability of optical imagery, offering a high temporal
433 coverage and a spatial resolution suitable for per-plot crop type mapping (Schreier and Dech,
434 2005). The increased availability of cloud-free images will facilitate the continuous refining
435 of the spectral-temporal profiles for common crop types and different agro-regions under cur-
436 rent climatic conditions and is expected to improve the classification accuracy of crop type
437 maps using these profiles.

438

439 ***Acknowledgements***

440 The research was funded by the German Federal Ministry of Education and Research in the project
441 “Management in the Havel river basin” (project funding reference number: 0330227). We thank To-
442 bias Schmidt for this help with the figures. The authors are grateful to two anonymous reviewers for
443 their comments that improved the quality of this paper.

444

445 **References**

446 Amt fuer Statistik Berlin Brandenburg, 2010. <http://www.statistik-berlin-brandenburg.de>. last accessed Novem-
447 ber 2011.

448 Blaschke, T., 2010. Object based image analysis for remote sensing. *ISPRS Journal of Photogrammetry and Re-*
449 *mote Sensing.* 65, 1, 2-16.

450 Bradley, B.A., Jacob, R.W., Hermance, J.F., Mustard, J.F., 2007. A curve fitting procedure to derive inter-annual
451 *phonologies from time series of noisy satellite NDVI data. Remote Sensing of Environment.* 106: 137-
452 145.

453 Castillejo-González, I.L., López-Granados, F., García-Ferrer, A., Pena-Barragán, J.M., Jurado-Expósito, M.,
454 *Sánchez de la Orden, M., González-Audicana, M., 2009. Object- and pixel-based analysis for mapping*
455 *crops and their agro-environmental associated measures using QuickBird imagery. Computers and*
456 *Electronics in Agriculture.* 68: 207-215.

457 De Witt, A., Clevers, J., 2004. Efficiency and accuracy of per-field classification for operational crop mapping.
458 *Int. J. Remote Sensing.* 25:20, 4091-4112.

459 Huete, A., 1988. A soil-adjusted vegetation index (SAVI). *Remote Sensing of Environment.* 25, 295-309.

460 Huete, A., Liu, H. Q., Batchily, K., van Leeuwen, W., 1997. A comparison of vegetation indices over a global set
461 *of TM images for EOS–MODIS. Remote Sensing of Environment.* 59, 440–451.

462 Huete, A., Didan, K., Miura, T., Rodriguez, E. P., Gao, X., Ferreira, L. G., 2002. Overview of the radiometric
463 *and biophysical performance of the MODIS vegetation indices. Remote Sensing of Environment.* 83,
464 195–213.

465 Jakubauskas, M., Legates, D., Kastens, J., 2002. Crop identification using harmonic analysis of time-series
466 *AVHRR NDVI data. Computers and Electronics in Agriculture.* 37, 127-139.

467 Krysanova, V., Müller-Wohlfeil, D.-I., Becker, A., 1998. Development and test of a spatially distributed hydro-
468 *logical/water quality model for mesoscale watersheds. Ecological Modelling.* 106, 2-3, 261-289.

469 Murakami, T., Ogawa, S., Ishitsuka, K., Kumagai, K., Saito, G, 2001. Crop discrimination with multitemporal
470 *SPOT/HRV data in the Saga Plains. Japan. Int. J. Remote Sensing.* 22:7, 1335-1348.

471 Murthy, C. S., Raju, P. V., Badrinath, K. V. S., 2003. Classification of wheat crop with multi-temporal images:
472 *performance of maximum likelihood and artificial neural networks. International Journal of Remote*
473 *Sensing.* 24:23, 4871-4890.

474 Odenweller, J.B., Johnson, K., 1984. Crop identification using Landsat temporal-spectral profiles. *Remote Sens-*
475 *ing of Environment.* 14: 39-54.

476 Panigrahy, S., Sharma, S.A., 1997. Mapping of crop rotation using multirate Indian Remote Sensing digital data.
477 *ISPRS Journal of Photogrammetry & Remote Sensing.* 52: 85-91.

478 Pantaleoni, E., Engel, B. A., Johannsen, C. J., 2007. Identifying agricultural flood damage using Landsat image-
479 ry. *Precision Agriculture*. 8, 1-2, 27-36.

480 Reed B.R., White M.A., Brown J.F., 2003. Remote sensing phenology. In *Phenology: An Integrative Environ-*
481 *mental Science* (ed Schwartz M.D.), pp. 365-381. Kluwer Academic Publishers, New York, NY.

482 Richter, R., 1996. A spatially adaptive fast atmospheric correction algorithm. *Int. J. Remote Sensing*. 17:1201-
483 1214.

484 Sakamoto, T., Yokozawa, M., Toritani, H., Shibayama, M., Ishitsuka, N., Ohno, H., 2005. A crop phenology
485 detection method using time-series MODIS data. *Remote Sensing of Environment*. 96, 366-374.

486 Schreier, G., Dech, S., 2005. High resolution earth observation satellites and services in the next decade—a Euro-
487 pean perspective, *Acta Astronautica*. 57, 2-8, 20-533.

488 Siebert, S., Ewert, F., 2012. Spatio-temporal patterns of phenological development in Germany in relation to
489 temperature and day length. *Agricultural and Forest Meteorology*. 152: 44-57.

490 Van Niel, T., McVicar, T., 2004. Determining temporal windows for crop discrimination with remote sensing: a
491 case study in south-eastern Australia. *Computers and Electronics in Agriculture*. 45, 91–108.

492 Vinciková, H., Hais, M., Brom, J., Procházka, J. Pecharová, E., 2010. Use of remote sensing methods in study-
493 ing agricultural landscapes – a review *Journal of Landscape Studies*. 3, 53-63.

494 Wardlow, B., Egbert, S., 2008. Large-area crop mapping using time-series MODIS 250 m NDVI data: An as-
495 sessment for the U.S. Central Great Plains. *Remote Sensing of Environment*. 112: 1096-1116.

496 Wardlow, B., Egbert, S., Kastens, J., 2007. Analysis of time-series MODIS 250 m vegetation index data for crop
497 classification in the U.S. Central Great Plains. *Remote Sensing of Environment*. 108, 290–310.

498 Wulder, M. A., White, J. C., Goward, S. N., Masek, J. G., Irons, J. R., Herold, M., Cohen, W. B., Loveland, T.
499 R., Woodcock, C. E., 2008. Landsat continuity: Issues and opportunities for land cover monitoring.
500 *Remote Sensing of Environment*. 112, 3, 955-969.

501 Yang, C., Everitt, J.H., Murden, D., 2011. Evaluating high resolution SPOT 5 satellite imagery for crop identifi-
502 cation. *Computers and Electronics in Agriculture*. 75: 347-354.

503

504 Tab. 1: Cultivation data collected from six agricultural companies between the years 1987-
505 2002 used for setting up the spectral-temporal profiles

Crop type	Total number of plots
Fallow	760
Field grass (perennial and first year)	120
Winter rye	890
Winter wheat	345
Winter barley	320
Oilseed rape	270
Summer grain	125
Sugar beets	60
Maize	365
Oilseed crops and legumes	325
Overall sum of plots	3745

506

507

508 Tab. 2: Acquisition dates of the 35 LANDSAT images sorted by the day of the year and re-
 509 spective crop development stages of winter wheat used for setting up the spectral-temporal
 510 profiles

Acquisition date of satellite image	Day of the year of image acquisition	Growth stage / agro-technical treatment
12.01.1989	12	Tillering (hibernation)
01.02.1996	32	Tillering (hibernation)
12.02.2000	43	Tillering (hibernation)
26.03.1998	85	Tillering
15.04.1988	105	Tillering
21.04.1996	111	Tillering
24.04.1997	114	Tillering
29.04.1987	119	Stem elongation
30.04.1999	120	Stem elongation
02.05.2000	122	Stem elongation
05.05.1995	125	Stem elongation
09.05.1988	129	Stem elongation
28.05.1992	148	Stem elongation
02.06.1997	153	Stem elongation
08.06.1996	169	Stem elongation
19.06.2000	170	Flowering
21.06.1998	172	Flowering
07.07.1989	188	Begin of yellow-ripeness
08.07.1995	189	Milk-ripeness
11.07.1999	192	Milk-ripeness
21.07.1994	202	Yellow-ripeness
09.08.1995	221	Shortly after harvest (stubbles)
11.08.1996	223	Yellow-ripeness
11.08.2002	223	Shortly after harvest (stubbles)
14.08.2000	226	Shortly after harvest (stubbles)
20.08.2002	232	Shortly after harvest (stubbles)
22.08.1994	234	After harvest
27.08.2002	239	After harvest
04.09.1987	247	After harvest
12.09.2002	255	After harvest
13.09.1999	256	After harvest
15.09.1991	258	After harvest
15.09.1997	258	After harvest
14.10.1996	287	Sowing
25.10.1994	298	Start of seeding development

511
 512

513 Tab. 3: Acquisition dates of satellite images and phenologically corrected days of year used
 514 for crop type classification for the growing season 1994/1995

Acquisition date of satellite image		25.10.1994	05.05.1995	08.07.1995	09.08.1995
Day of year of image acquisition		298	125	189	221
	Fallow	293	132	184	226
	Perennial field grass	293	132	184	226
	Winter rye	298	128	193	221
	Winter wheat	293	132	184	226
	Winter barley	298	135	189	221
	Oilseed rape	298	135	183	221
	Summer grain		125	183	225
	Sugar beets		128	191	224
	Maize		128	189	218
	Oilseed crops and legumes		125	183	225
	Potatoes		128	191	224
	First year field grass		125	183	225

515

516

517 Tab. 4: Error matrix for classification based on NDVI temporal profiles using four images of
 518 the growing season 1994/1995

		Classification results														
Reference data		Fallow	Perennial field grass	Winter rye	Winter wheat	Winter barley	Oilseed rape	Summer grain	Sugar beets	Maize	Oilseed crops and legumes	Potatoes	First year field grass	Area in ha	Correctly classified area in ha	Errors of omission (ha, %)
	Fallow	76.6	1.6	0.4			6.7	1.6		0.4	4.4	3.2	5.1	328.6	251.7	76.9 23.4
	Perennial field grass													0	0	0
	Winter rye	10.1		71.1	8.8	6.1	1.6				0.4	1.9		299.0	214.1	84.9 28.9
	Winter wheat	1.6		2.9	91.7		1.5	0.7					1.6	214.0	196.2	17.8 8.3
	Winter barley	5.3		10.8		76.9	3.9				2.0	1.1		186.4	143.3	43.1 23.1
	Oilseed rape	1.2			1.5		97.3							67.5	65.7	1.8 6.7
	Summer grain				52.4		47.6							54.0	0	54.0 100
	Sugar beets										100.0			27.7	0	27.7 100
	Maize	0.4		6.2	1.4		1.3	0.6		14.5	1.8	68.5	5.2	271.0	39.5	231.5 85.5
	Oilseed crops and legumes	2.1					1.0			3.1	92.1	1.7		167.5	154.3	13.2 7.9
	Potatoes													0	0	0
	First year field grass		100.0											3.7	0	3.7 100
	Area in ha	300.9	9.1	257.4	255.6	161.6	133.6	8.4	0	45.5	206.2	206.8	34.2	Σ 1619.4*	1064. 7	
	Correctly classified area in ha	251.7	0	214.1	196.2	143.3	65.7	0	0	39.3	154.3	0	0	1064.7	Overall Accuracy	
	Errors of commission (ha, %)	49.2 16.4	9.1 100	43.3 16.8	59.4 23.2	18.3 11.3	67.9 50.8	8.4 100	0	6.2 13.2	51.9 25.2	206.8 100	34.2 100			65.7 %

* overall validation area

519

520

521

522 Tab. 5: Error matrix for maximum likelihood classification using four images of the growing
 523 season 1994/1995

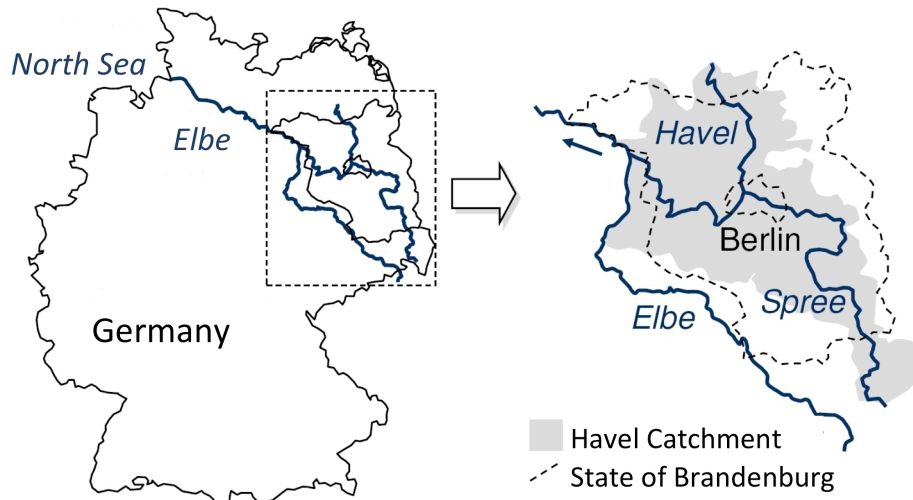
		Classification result															
Reference data		Fallow	Perennial field grass	Winter rye	Winter wheat	Winter barley	Oilseed rape	Summer grain	Sugar beets	Maize	Oilseed crops and legumes	Potatoes	First year field grass	Area in ha	Correctly classified area in ha	Errors of omission (ha, %)	
	Fallow	78.6	3.5	0.4	8.7	1.8			0.3	6.6					328.6	258.3	70.3 21.4
	Perennial field grass													0	0	0	
	Winter rye	11.0	2.3	68.2	5.2	2.5	3.9	6.3						299.0	203.8	95.2 31.8	
	Winter wheat			2.9	95.5		0.9			0.7				214.0	204.5	9.5 4.5	
	Winter barley	2.0	4.2	5.0	3.7	71.7	12.3			1.1				186.4	133.6	52.8 28.3	
	Oilseed rape				5.2		94.8							67.5	64.0	3.5 5.2	
	Summer grain						27.8	72.2						54.0	39.0	15.0 27.8	
	Sugar beets								100.0					27.7	27.7	0.0 0.0	
	Maize	1.8		4.4	2.1		3.2		23.8	64.6				271.0	175.1	95.5 35.4	
	Oilseed crops and legumes	1.4	47.7		1.0		1.0		1.0	4.7	43.2			167.5	72.3	95.2 56.8	
	Potatoes													0	0	0	
	First year field grass		67.6				32.4							3.7	0.0	3.7 100	
	Area in ha	305.7	57.9	232.9	268.3	147.1	125.9	106.1	94.8	208.2	72.3	0	0	Σ 1619.4*	1178.3		
	Correctly classified area in ha	258.3	0	203.8	204.5	133.6	64.0	39.0	27.7	175.1	72.3	0	0	1178.3	Overall Accuracy		
	Errors of commission (ha, %)	47.4 15.5	57.9 100	28.1 11.1	63.8 23.8	13.5 10.1	61.9 53.3	67.1 63.2	67.1 70.8	33.1 15.9	0.0 0.0	0	0		72.8 %		

524 * overall validation area

525

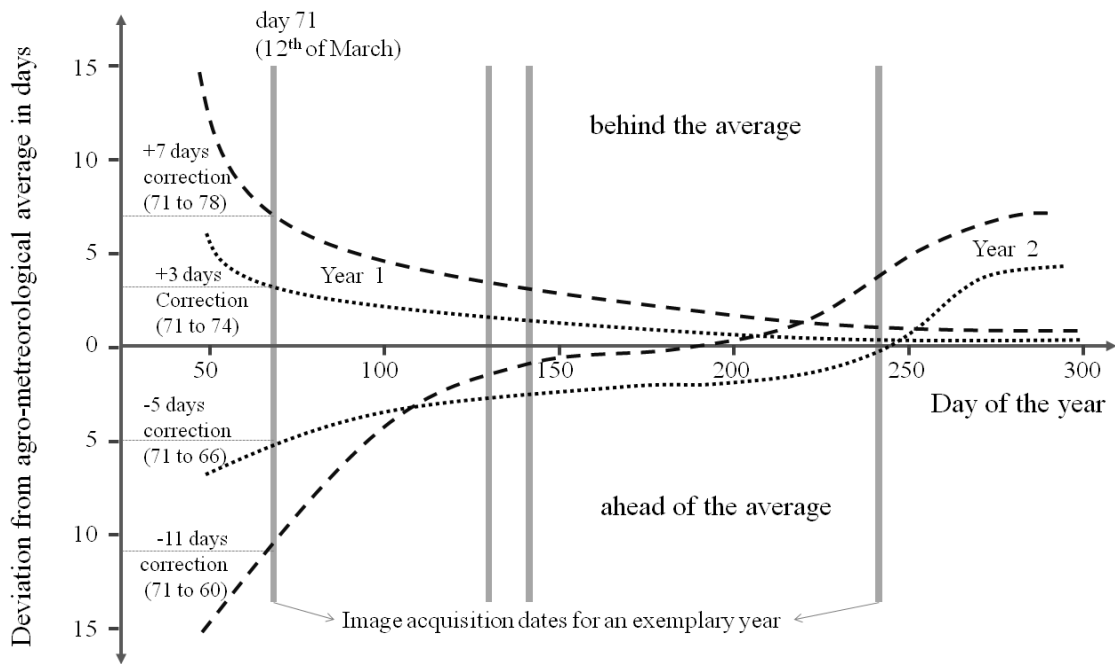
526

527



528
529 Fig. 1: Location of study area

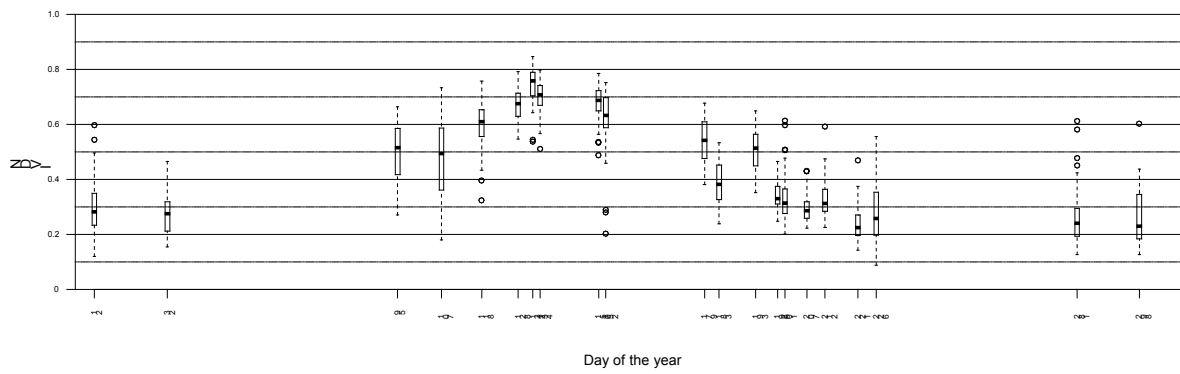
530



531

532 Fig. 2: Schematic graph of the phenological correction for two different years (marked as
 533 Year 1 and Year 2). Dotted and dashed lines represent the deviation from the average year in
 534 days for two different crop types. Positive values indicate a delayed crop development, nega-
 535 tive values a crop development ahead of the average.

536

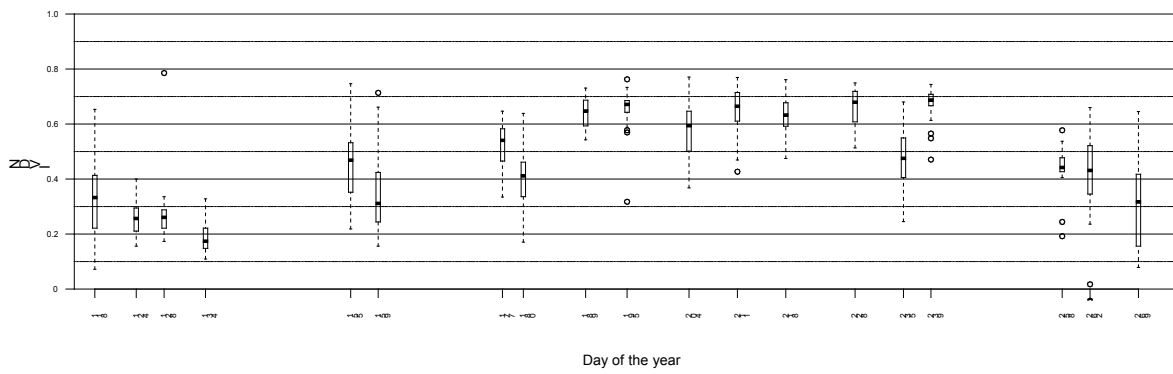


537

538 Fig. 3: NDVI response during the growing season of winter rye. Whiskers represent the 1.5
 539 times interquartile range and the dots represent outliers.

540

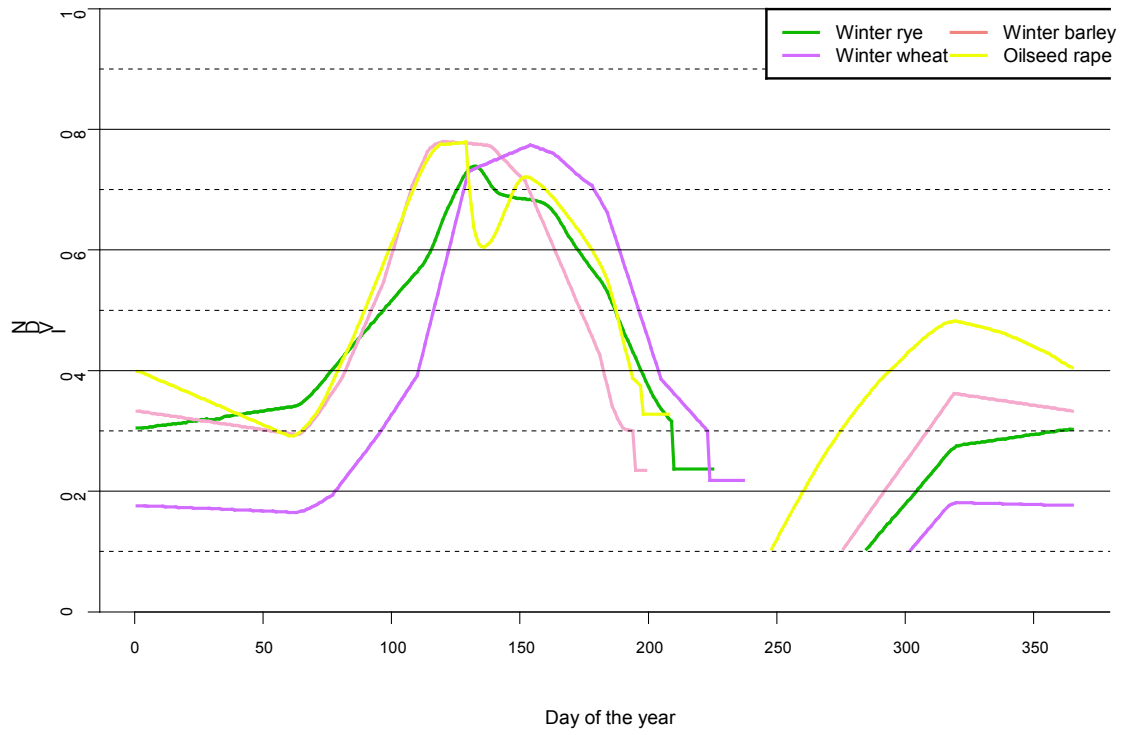
541



542

543 Fig. 4: NDVI response during the growing season of maize. Whiskers represent the 1.5 times
544 interquartile range and the dots represent outliers.

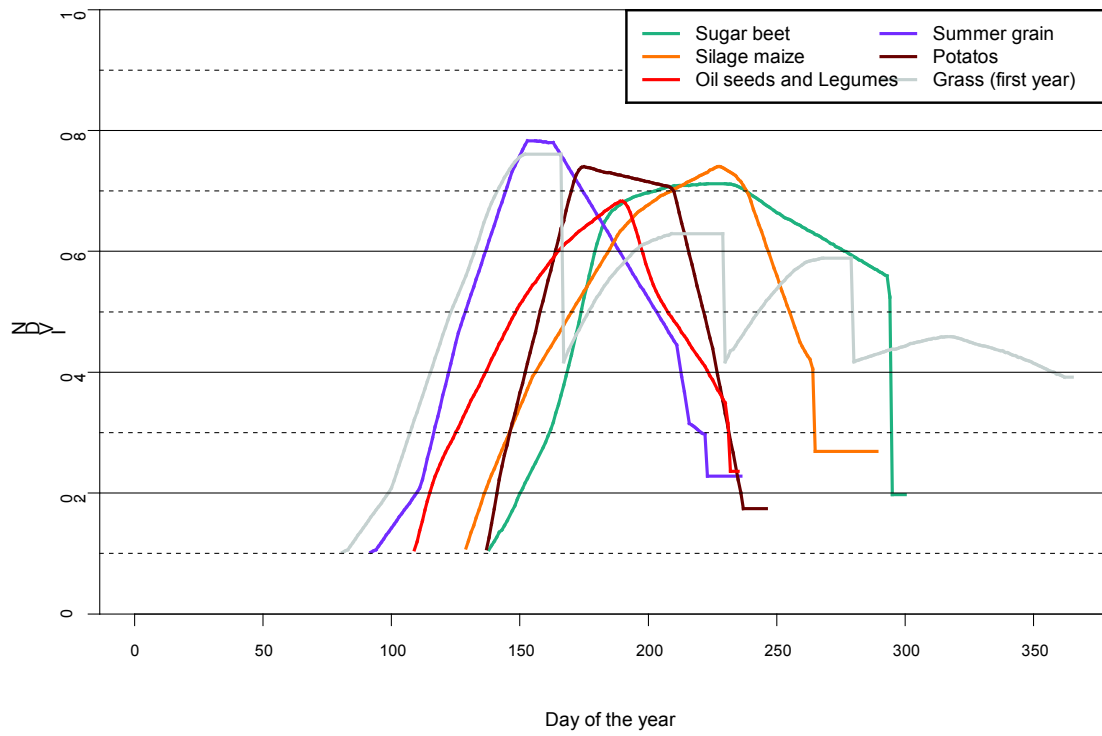
545



546

547 Fig. 5: NDVI temporal profile of winter crops

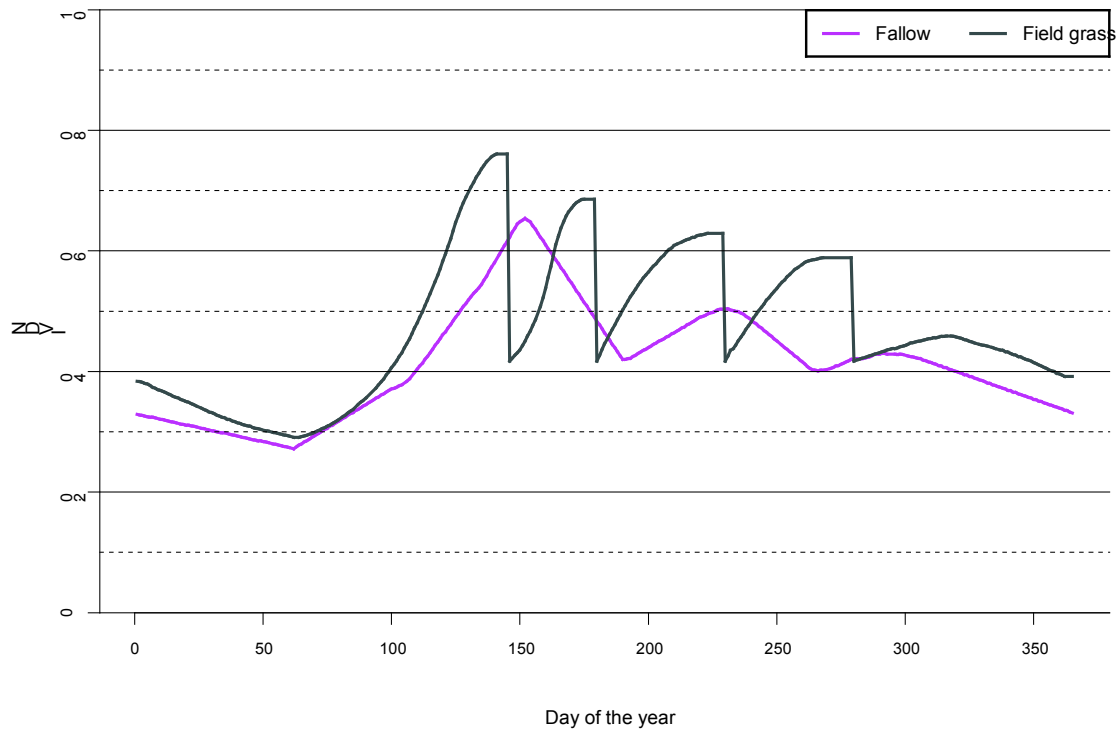
548



549

550 Fig. 6: NDVI temporal profile of summer crops

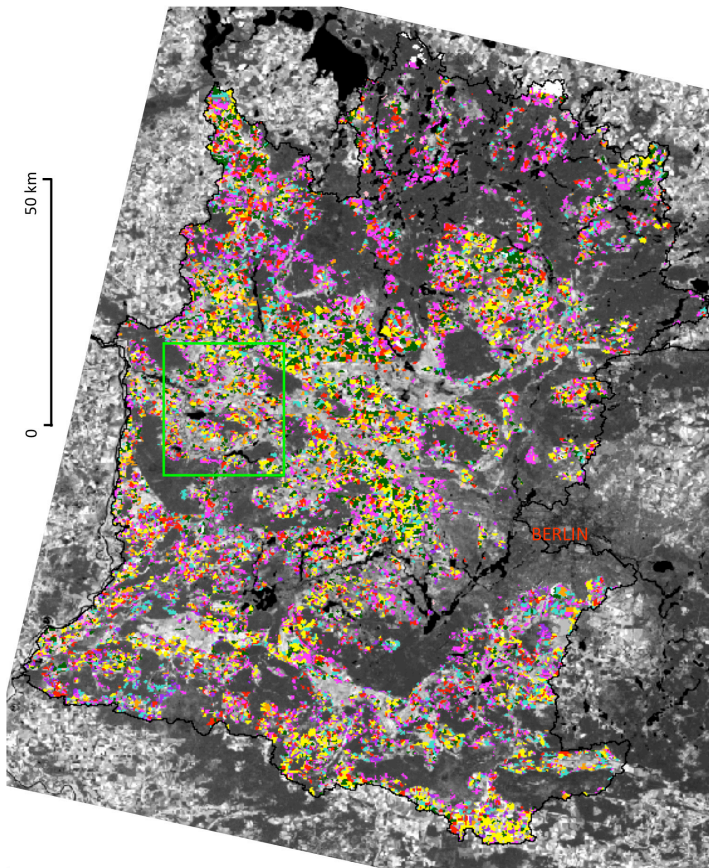
551



552

553 Fig. 7: NDVI temporal profile of perennial field grass / fallow land

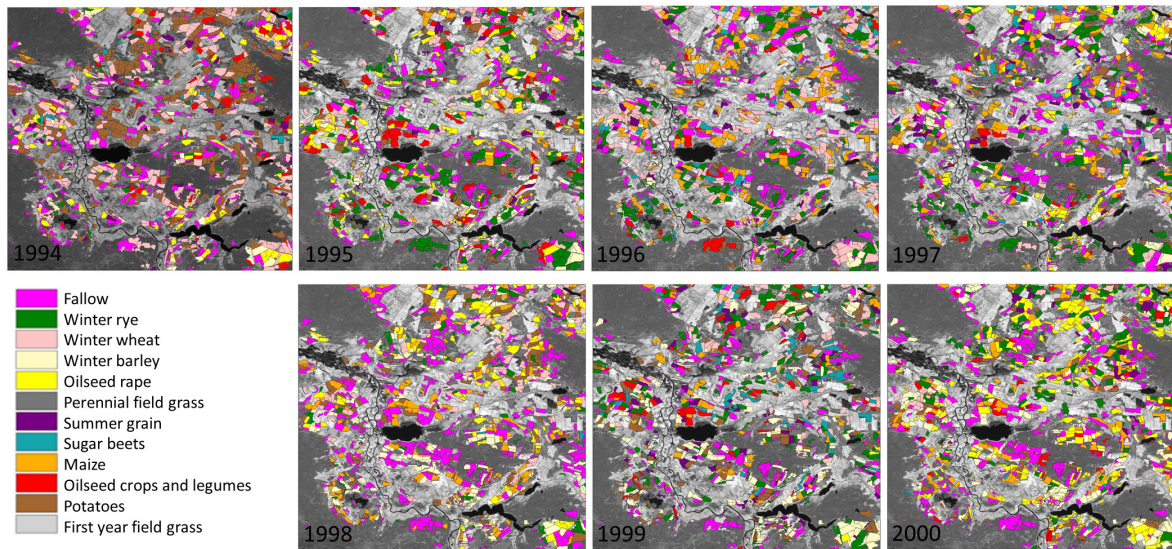
554



555

556 Fig. 8: Crop type map of the entire study area for the year 2000, subset region (Fig. 9) marked
557 in green. For legend refer to Fig. 9.

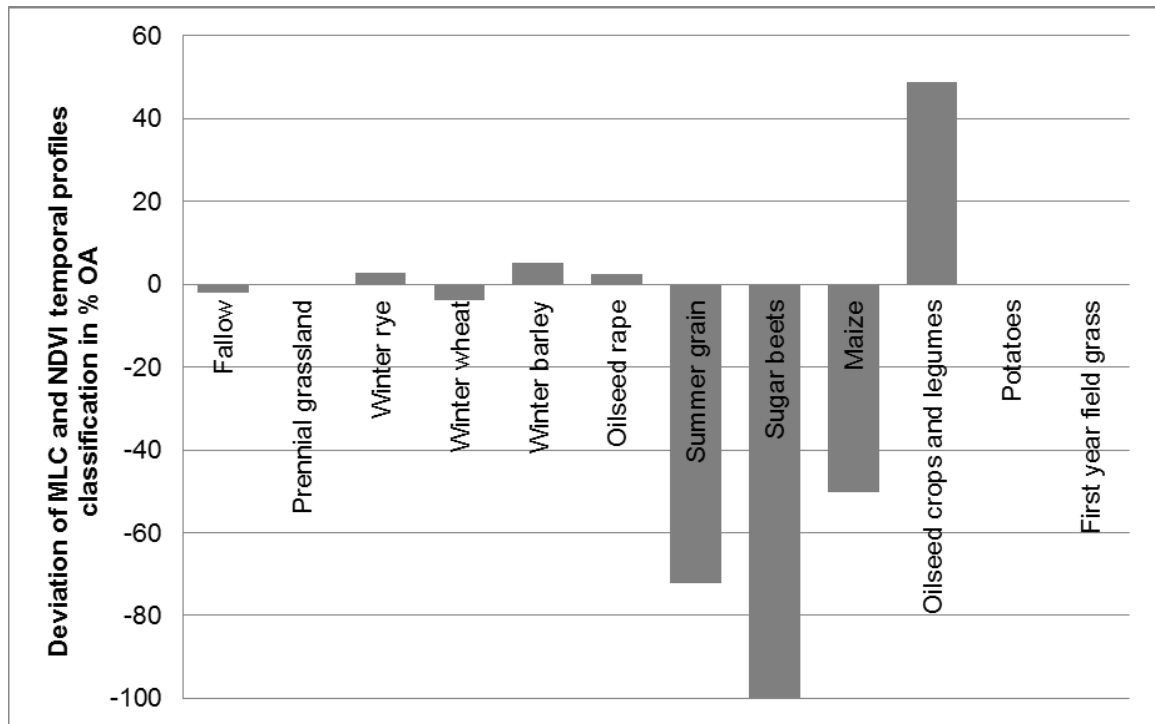
558



559

560 Fig. 9: Crop type maps for a subset region for the years 1994-2000

561



562

563

564

565

566

567

Fig. 10: Deviation of the overall accuracy (OA) between maximum likelihood classification (MLC) and spectral-temporal profiles classification per crop type class for the growing season 1994/95. Positive values indicate higher overall accuracies of the spectral-temporal profiles classification.